Geophysical and Geodetical Investigation of A Landslide Area (Koyulhisar-Sivas, Turkey)

Sevda Özel[1], Demet Över[2], Kemal Ö. Hastaoğlu[3]

[1,2]Department of Geophysical Engineering, Cumhuriyet University, 58140, Sivas, Turkey
[3]Department of Geomatics Engineering, Cumhuriyet University, 58140, Sivas, Turkey

Correspondence to: Sevda Özel (sozel@cumhuriyet.edu.tr.)

Abstract. The study area is in the west of Koyulhisar (Sivas) town center and approximately 200x250 m^2. This area is one of the most active locations where the landslide displacement amount is the greatest. The aim of this study is to determine the depth of the sliding surface with geophysical (seismic refraction tomography (SRT), ground-penetrating radar (GPR)) methods. The results of TÜBİTAK-111Y111 project were also used. According to the geophysical results, within ~20 m of investigation depth, three layers with the average seismic P-wave velocities (V_P) of 650, 1200 and 2100 m/sec were identified. It was determined that the depth of the sliding surface which was between ~3-7 m and the seismic velocities were lower than 650 m/sec from these depths to the surface. The geophysical results demonstrated that the landslide type was identified as planar sliding, with the sliding direction in S-SE, and the tilt of the geological layer was in the same direction with the topography slope, mostly bigger than 5°. It was observed that the deformations in the landslide mass were caused by the geological unit, the layer or topography slope, and precipitation. All of these results can be effective in triggering the landslide area in the future and the landslide activity may continue in the study area. Therefore, the study area contains the risk and the natural hazards, and these threaten the settlement area and other constructions in Koyulhisar.

1 Introduction

A landslide is a mass movement and can occur in different forms. Koyulhisar landslide area is one of the largest landslide areas, significantly, leading to serious loss of lives and property, in Turkey. Three of the most destructive of these landslides occurred in Koyulhisar (Sivas) on 19 August 1998, 20 July 2000 and 17 March 2005. The Koyulhisar landslide area is one of the most important large landslide areas in the country and mass movements there typically occurs in the form of debris or mudflow (Tatar et al., 2007; Duman et al., 2005). Koyulhisar is also an active landslide area and for the past 17 years, there has been observed an increase in landslide activity (Tatar et al., 2007; Över, 2015). The large and small landslides in Koyulhisar landslide area have mostly occurred due to natural causes until today. Artificial causes mainly constitute the landslides caused by human interventions (blasting, drilling, improper planting, loading, loss of vegetation cover, etc.). The last large landslide occurred with the flow of mud in the north of Koyulhisar landslide area in March 2005. Duman et al. (2005) determined that this landslide was in the excessively fast (6 m/sec) class. Demirel et al. (2016), for the landslide in 2000 years revealed an average of 2.5-7.4 mm/year slip rate. Researchers have stated that these landslides usually have a mechanism involving a circular rotation, this old landslide mass maintains its activity and partial landslides occur on the groundmass (Sendir and Yılmaz, 2001; Duman et al., 2005). Therefore, Koyulhisar district center is on an old landslide that occurred in the form of circular rotation. The front of this landslide mass is open, it is always active, activity is not massive and usually in the form of local landslides occurring on the groundmass (Sendir and Yılmaz, 2001).

The triggering mechanisms of landslides are often complex and further understanding is needed to facilitate the prediction of mobilizations as well as adequate stabilization and remediation measures. Therefore, it is important to investigate the reasons that affect the formation mechanisms and the formation of landslides. Different engineering (geology, geophysics, geodetic, etc.) disciplines have great role and importance especially in decreasing the landslide effects. They can help to prevent damage by prediction and early warning. In this context, Koyulhisar landslide area was examined in a wide area with detailed global navigation satellite system (GNSS) methods and the studies of other disciplines (geology, geochemistry, seismology, meteorology, remote sensing) (Sendir and Yılmaz, 2002; Tatar et al., 2007; Hatiboğlu, 2009; Hastaoğlu and Şanlı, 2011; Yılmaz, 2009; Hastaoğlu, 2013; Topal and Hatiboğlu, 2015; Hastaoğlu, 2016; Hastaoğlu et al., 2018). The annual sliding velocity, sliding direction, displacement amounts and natural disaster risk of the landslide have been identified by these studies. It has been determined that the displacement amounts of the landslide velocity vary between 1-8.6 cm/year by topography and geological bedding and that the landslide direction is usually S-SE oriented. In terms of geology, some researchers have carried out geological studies on many issues such as geological, tectonic, geotechnical, geochemical and geomorphological studies at the local and regional scale in which the features of the faults, water, hot water, soil and rock on the North Anatolian fault zone (NAFZ) and in the region were investigated. These studies are in geology, tectonics (Toprak, 1989; Uysal, 1995; Sendir and Yılmaz, 2001; Sendir and Yılmaz, 2002; Yılmaz et al., 2005; Gökçeoğlu et al., 2005b; Demirel et al., 2016; Demir, 2018), and geotechnics, geomatics/remote sensing, geochemistry and geomorphology (Toprak, 1989; Uysal, 1995; Duman et al., 2005; Ulusay et al., 2007; Hatiboğlu, 2009; Yılmaz, 2009; Demirel et al., 2016; Demir, 2018). At the interpretation stage, the geophysical findings of this study are related to the results of all these studies mentioned just above.

The geophysical studies were carried out in a limited area where the first geophysical studies took place. In particular, seismic tomography (seismic refraction tomography (SRT), multi-channel seismic wave analysis (MASW)) and ground-penetrating radar GPR applications are preferred methods in landslide studies. The structural geometry of the landslide area was delineated based on an interpretation of the collected geophysical data. These are the seismic V_P velocities, thickness, tilt and direction of the layers. Thus, other features such as the sliding surface depth of the landslide, landslide type, advancement direction, and the risk situation were also revealed, and geophysical and other study results were shown to be compatible with each other. The studies carried out by McCann and Forster (1990), Demirağ (1991), Hack (2000), Perrone et al. (2004), Göktürkler et al. (2008), Hu and Shan (2016), Su et al. (2016) and (Popescu et al. 2016) are important in this regard. In addition, Bichler et al. (2004) carried out multi-methodical geophysical studies containing electrical resistivity, GPR and seismic methods in the landslide studies. Otto and Sass (2006) and Ristic et al. (2012) also carried out similar studies on landslide investigation. In these studies, the sliding surface of the landslides and the flow direction properties of the landslide material were generally determined by 2D (two-dimension) and 3D (three-dimension) geophysical sections.

It has been observed that the use of the SRT and GPR methods in landslide studies has increased in recent years (Ristić et al., 2012; Timothy et al., 2013; Lissak et al., 2015; Hu and Shan, 2016; Popescu et al., 2016; Su et al., 2016). The parameters which define the landslide such as landslide geometries and bedrock depth or sliding surface depth have been determined in these studies. Regarding the GPR method, significant studies have been carried out by Davis and Annan (1989) on revealing the soil stratigraphy, by Aldaş et al. (2003), Slater and

Niemi (2003) and Green et al. (2003) on the mapping of faults, fractures and cracks and by Benson (1995), Harari (1996), Bano et al. (2000) and Bubeck et al. (2015) on the determination of groundwater levels. However, the accurate determination of the landslide type is also very important as well as landslide elements. Joint studies with geophysics and other disciplines are commonly carried out in determining the landslide type and for different contributions. In addition to these, the seismological history, morphological and topographical features and meteorological data of the study area are always taken into account in the landslide analysis. These data are used to contribute to the interpretations of these studies. Thus, through multi-discipline studies, the landslide type can be determined most accurately by determining different sliding behaviors (such as the velocity and direction of the landslide, annual amount of displacement) varying from region to region. The landslides, which generally occur in the form of sliding, may occur with the movements of falling, sliding and flowing or with the combination of a few of these. Therefore, accurate determination of the landslide type and the selection of the methods used in the study is very important. It may be possible to perform an accurate landslide analysis only if these requirements are met. In this article, these issues were examined and discussed separately and together with geophysical and geodetic results.

2 The Status of the Study Area

2.1 Geology and seismology

Koyulhisar is about 180 km away from Sivas city center. The study area is located in the west of Koyulhisar town center and in the north of the NAFZ (Fig. 1). The geological investigation of Koyulhisar has been carried out regionally or locally by various researchers (Terlemez and Yılmaz, 1980; Toprak, 1989; Uysal, 1995; Sendir and Yılmaz, 2002; Duman et al., 2005; Hatiboğlu, 2009). In these studies, the Plio-Quaternary aged Koyulhisar Formation is the youngest unit in the region. It was stated that the youngest unit consisted of the talus (slope or deposit) and fluvial conglomerates and was seen along the strike-slip faults (Toprak, 1989). Toprak (1989) divided the NAFZ which is represented by a right lateral strike-slip fault zone into five fault sets including the North Anatolian Main Fault, Koyulhisar fault sets, Kelkit fault set, Şıhlar fault set and Kuruçay fault set. But, the Şıhlar fault sets affect Koyulhisar district center at the nearest (Fig. 1). Toprak (1989) stated that Koyulhisar section of the NAFZ is still active and a right lateral strike-slip fault zone due to the morphotectonic structures and seismic activities in the region (Fig. 1 and 2). As it is seen in Fig. 1, the faults closely concerning Koyulhisar are the NAFZ, which is the main fault extending in the northwest-southeast direction and approximately 2-2.5 km away, in the south, and the Çamlıyaka Fault, which is approximately north-south-oriented, in the west. This fault which is the closest one to the study area extends perpendicular to the NAFZ in the south. It was also reported by Tatar et al. (2007) that large and old landslide masses in Koyulhisar landslide area have lower Miocene-aged clay and gypsum levels, Eocene-aged clayey levels and Plio-Quaternary aged sediments. The rocks in the region usually have fractures and discontinuities and are crushed because of the NAFZ which is tectonically active in the south of the study area (Tatar et al., 2005). There are also many old and new landslides in the study area depending on the high tilted topography. For these reasons, the directions of movement of the landslides generally threaten the settlement areas (Sendir and Yılmaz, 2001). However, Hatiboğlu (2009) and Hastaoğlu et al. (2015) generally observed two geological units in the drillings in the study area. They observed that the upper unit was silty sandy clay and sand interbedded silty clay in some places up to about 10 m, and advanced as sand interbedded silty clay and sand interbedded clay in some places towards deeper than 10 m. The first unit consists of light-dark brown colored, medium-very stiff, low-high plasticity, silty clay. The second unit consists of light-yellow white colored, low-high plasticity, silty sandy clay interbedded with sand (Hastaoğlu et al., 2015). When the drilling logs are examined, there is generally the second unit in east of study area (Hastaoğlu et al., 2015). Furthermore, it was observed that the content of the second geological unit did not change even if the depth of the drilling increased. Therefore, the second geological unit was taken into consideration in the interpretation of geophysical sections.

As it is seen in Fig. 2, the study area is located in an active area in terms of seismicity (Fig. 2). The seismological history, the magnitude (M) of which is greater than 2.5, of the examined area and its surrounding were investigated for this article. Fig. 2 was prepared with the seismological data between 1900-2015 (UDİM, 2016). Particular attention was paid to the earthquakes before 2005 in the seismological interpretation. This is because the largest and most recent landslide occurred in the area in 2005 and it was aimed to investigate its relationship with displacements and previous landslides. The type of magnitude which is calculated from seismological data is usually the local magnitude. The depths (d) of these earthquakes with higher M>2.5 vary between approximately 5 and 80 km (Fig. 2). According to the seismic data of the years examined, Koyulhisar and its surroundings have always been active seismically. It was observed that this frequency of earthquakes usually occurred on the NAFZ in the south of the study area. Additionally, it has been analyzed the seismic activity of the region at least for the last 112 (1904-2016) years by Demir (2018). In this study, he express that the most notable is probably the relationships between the magnitude of the earthquake to the number of landslides and the area affected by the landslides and between the magnitude and the maximum distance of landslide observations from the epicenter in different geological, topographical, and climatic conditions (Demir, 2018).

Large earthquakes affecting Koyulhisar district also occurred in the region. These largest earthquakes are in the south of the NAFZ or Suşehri district and a total of three large earthquakes with M≥5.6 occurred there (Över, 2015). Among these, the 1992 earthquake is closest to the study area with the least depth but the second largest earthquake (Fig. 2). This earthquake is an earthquake with 6.1 magnitudes that occurred 10 km below the ground. The large earthquakes in the south of Suşehri district which is just 13 km away from the study area occurred in 1909 and 1939. 1909 earthquake occurred 60 km below the ground and is the largest and deepest earthquake with a magnitude of 6.3. 1939 earthquake is also deep and the third largest earthquake that occurred 50 km below the ground with a magnitude of 5.6 (Över, 2015). In addition, when Fig. 2 is analyzed, it is seen that the magnitudes of the other earthquakes in the north of the NAFZ and the upper elevations of the landslide generally vary between 2.5-4. Similarly, it is seen that the other earthquakes in the south of the landslide area are the earthquakes with a magnitude of greater than 3.6. All these earthquakes may have triggered the landslide mass from time to time in places where sliding surfaces, layers, and topography in the landslide area are more inclined than 5-10 degrees (according to the geophysical cross-sections in this article, when it is considered that there are loose units and deformations on the sliding surfaces). In particular, they further affected the landslide mass along with the rain and caused large amounts of displacement in the landslide area.

2.2 Meteorological and geodetic results

The data regarding the rainfalls with the effects of triggering the landslides are presented in Table 1 and Fig. 3a and Fig. 3b (MGM, 2016; Hastaoğlu et al., 2015). With these data, the rainfall status of the study area and its surrounding was examined by months as average annual rainfalls and the annual areal amount of rainfall. According to the data obtained between 1950-2015 in Table 1, the rainy periods are generally between October-

November-December and January-February-March-April. The highest total daily amount of rainfall in the rainiest years was observed as snowfall in 1950 (110 cm) and as rain in 1991 (55 kg/m^2). In Fig. 3a, the annual normal average rainfall value calculated for the years between 1981-2010 was calculated as over 483.4 mm (MGM, 2016). However, 1987-1988 and 1997-1998 were the rainiest years. It is seen that the annual areal amount of rainfall exceeded the normal values and was higher than 550 mm in these rainy years that took place in every 10 years. Similarly, it is also seen that there were high rainfalls for 3-4 years after the years of 1985-1995-2005 with an interval of 10 years. Therefore, annual areal rainfalls were observed to be more before some large landslides like the landslide in 1998. When geological features of the region are taken into account, it is remarkable that the landslide in 1998 and 2000 occurred in the summer months after the winter with a heavy fall of snow. However, the landslide in 2005 occurred during the rainy season.

In Fig. 3b, GNSS studies and multi-disciplinary studies of Hastaoğlu et al. (2015) have carried out for many years (about 6 years) to determine the deformation and annual sliding amounts especially after the landslides in 1998-2000-2005. The seismological and meteorological data, which were updated by the geodetic (GNSS (DH), geological (IDH (Inclinometer Drilling Holes)) and meteorological data collected in this local study were reorganized and evaluated. Fig. 3a-b and Table 1 which were reprepared for the study which is the subject of this article were associated with the results of GNSS studies (Fig. 3b). The monthly and annual meteorological data should certainly be evaluated particularly within the scope of monitoring activities, as the area is a landslide area. Hastaoğlu et al. (2015) followed in DH wells in the area in 2013-2014 (Fig. 3b). If Fig. 4 is examined, there are seven DH point in the nearest of the geophysical profiles (DH8, DH12, DH16 is near the area A and DH4, DH6, DH9, DH10 is near the area C). The graphics in Fig. 3b was prepared from the combined data (unpublished data in the project) and the temperature (^{0}C), precipitation (m^3) and soil moisture content (cm) were compared in these graphics. The temperature and precipitation were observed to be inversely proportional during the summer months called as a dry period. It is seen that the soil moisture is changeable apart from the rainy period and has very high water content during the rainy periods. The soil moisture is very high (average 150 cm) in winter, summer, autumn seasons. In the study area, the water contents in the drilling data change from 24.6 % to 13.3 % at between 0-10 m depth and these values are also high (from 29.1 % to 17.3 %) after 10 m (Hastaoğlu et al., 2015). Water generated from precipitation and melting snow is blocked by the impermeable layer when it infiltrates downward, and the local moisture content increases (see Hu and Shan (2016)). Thus, the water infiltrates the interface between the permeable and impermeable layer, can form a slip zone. Then, these results were compared with geophysical results in interpretation. The GPR results show that the moisture content of soils at the sliding surface of the landslide mass is relatively high. The drilling data and soil moisture values also show very high moisture content of the sliding surface of the landslide mass in the study area, which is completely consistent with the results obtained from the GPR-SRT profiles, meteorological and geological results. On the other hand, it was understood that the precipitation increased by the decrease in temperatures. It is also seen that the total annual amount of rainfall increased about 2-fold in 2014 compared to 2013 (Fig. 3a-b). According to all results, rainfalls are considered to be effective in triggering of the landslide because the ground of this landslide area, which is filled with loose units and old cracks, is supersaturated with water due to the rainfalls. Besides, Hastaoğlu et al. (2015) determined that the groundwater level gets close to the surface for 4-6 m on average at the end of the rainy period, to 10 m at the end of the rainy period and decreases up to 25 m in some wells in the area where geophysical study area is also located, and the groundwater flow direction is SW.

Consequently, when the displacements and the landslide directions estimated from the GNSS measurements are also considered, it was determined that these results were compatible with the geophysical sections and the rainfalls were among the reasons that trigger the landslide.

3 Methods

3.1 Geophysical surveys

The seismic refraction tomography (SRT) and ground-penetrating radar (GPR) methods are applied in tomography format. The SRT method determining the seismic P-wave velocities (V_P) for seismic applications and the GPR method for electromagnetic (EM) applications were used in the geophysical data collection in the area (Fig. 4). The high-frequency electromagnetic waves can reach deeper in the environments with low conductivity like sand. However, the conductive units such as clay and shale decrease the penetration depth of the signal transmitted and lead to absorption (Annan et al., 1988; Davis and Annan, 1989). Firstly, SRT and GPR data were collected along multiple transects in two different areas of the study area named A and C (see Fig. 4). Then, the geophysical profiles were processed to the satellite map according to the coordinates along with the topographical elevation curves and GNSS measurement locations for the ease of interpretation (Fig. 4a). Geophysical measurements were taken due to the geologic bedding and topographic features (Fig. 4b-c). SRT profiles and on these seismic profiles GPR profiles in the area defined by A in Fig. 4b is approximately in the NE-SW (SRT2, SRT4, GPR2, GPR4)) and NW-SE (SRT3, SRT5, GPR3, GPR5) directions (Fig. 4b). Similarly, in area C, SRT11-SRT12-GPR11-GPR12 profiles are approximately in the E-W directions, SRT9-SRT14-GPR9-GPR14 profiles are approximately in the NE-SW direction, SRT10-GPR10 profiles are in the NW-SE directions and SRT13-GPR13 profiles are approximately in the NE-SW directions (Fig. 4c). The profile lengths usually range from 25 to 60 m according to the method applied.

The profile shooting technique in the seismic study, hammer and iron plate of 8 kg weight as the source P geophone of 14 Hz (the total number of geophones is 12) and Geometrics branded seismic device as the receiver was used while collecting the SRT data. In all profiles, the geophone interval was 5 m, offset distance was 2.5 m, the sampling interval was 256 ms and the record length was 512 ms. The geophones were respectively fixed on the ground within the selected geophone range and their connections with the seismic device were made. Then, seismic measurements were recorded by starting from the offset distance of 2.5 m, reducing to sledgehammer plate and making at least 5 times shots between each geophone, respectively. In the evaluation of the SRT data collected in the field, SeisImager program was used for displaying, processing and evaluation of the seismic refraction waves. The marking of the first arrivals of the SRT data was performed using Pickwin, and the evaluation of the first arrival data was performed using Plotrefa module. The GPR data were collected by Ramac2 device using a shielded antenna of 250 MHz. The GPR data were processed in Reflexw program. In order to collect the GPR data, other parameters were selected 512 ns-number of samples, 16-number of stacking and 0.1 m-trace interval. 2D GPR data processing for data analysis of the GPR data, it includes Static correction (10 ns in dry or wet clay and sandy), Muting, Bandpass filter (100, 200, 300, 400 Hz), Gain (0.512 ms) and Migration (0.01 ms) steps. The migration was made to show up small vertical structures invisible during data processing. Thus, very large hyperballs with strong reflections may limit the display of non-migrated GPR data. Moreover, the peak points of hyperbolas observed in GPR cross-sections show the reflection surface of the electromagnetic wave. During data processing, velocity analysis was performed on the reflection surfaces through the hyperbola superposition method and EM wave propagation velocity was calculated in all GPR cross-sections. The topographic corrections were made by selecting the "Correct for two layers" option in Static Correction/Muting in the Reflex program. The height values collected in the study area were manually entered and saved in the "Correct for two layers" option. Thus, the models were converted from m to ns and the GPR sections were prepared for interpretation. Thus, the collected geophysical data were converted into 2D (two-dimension) elevation-distance (SRT) and depth-distance (GPR) sections by assessed in the appropriate software.

The geophysical study area is one of the most active locations of the landslide area. As it is seen in Fig. 5, geomorphologically the landslide cracks on the surface, displacement traces, and structural damages in the study area and its immediate surroundings can be monitored clearly in this activity area. Visibly, the damaging effects of still active or old landslides on residences, roads and walls are also observed easily by field observations. Therefore, none of the damaged constructions are used in the Koyulhisar.

3.2 Geophysical analysis, results and discussion

Geophysical interpretations were made according to these sections and compared with the results of the other studies.

SRT sections: 2D seismic cross-sections giving seismic V_P-depth information are presented in Fig. 6 and 7. In the seismic data evaluation, the coincidence was provided with RMS (Root Mean Square) errors ranging between 3.4-4.5% in 2D inversion operation. According to these sections, two or three layers were identified at about 20 m depth (Fig. 6 and 7). It was understood that the tilts of these layers were southeast oriented, and their tilt was greater than 5^0. According to the average seismic velocities (V_P) calculated, three layers with the layer velocities of 650, 1200 and 2100 m/sec were defined from top to bottom. Thus, the seismic V_P velocities were observed that they increased towards the depth. It was determined that the depth of the sliding surface varied about between 3-7 m (Fig. 6 and 7). Therefore, these depths were defined as the layer with the risk of dislocation. This area was considered to have a risk of dislocation due to these loose units, rainfall and tilt conditions. The seismic velocity of the first layer is lower than V_{P1}<650 m/sec, but the seismic velocity of the third layer may be greater than V_{P3}>2100 m/sec.

GPR sections: The investigation depth was further calculated from the SRT sections compared to the GPR sections due to the differences of geophysical methods in the application. Because GPR sections were obtained in high-resolution for about the first 10 m depth after data processing of the GPR data. It is clearly observed that the strong reflections are within 10 m depth in Fig. 8 and 9. These strong reflections seen in black dashed ellipses are interpreted as deformation areas in the layer. In a similar manner, these areas being interpreted as deformations were also observed in the studies of Bubeck et al. (2015), Hu and Shan (2016), Su et al. (2016) and Popescu et al. (2016). The strong reflected wave signal shows distinctive characteristics, presenting a low-frequency high-amplitude sync-phase axis, which can be inferred as the sliding surface in Fig. 8 and 9. In other words, two layers were identified in GPR sections. The first layer is weak, loose, cracked, moved and also have lost their tightness, and their seismic velocity is low. Therefore, in Fig. 8 and 9, it was thought that deformations developed on the sliding surfaces due to the geology of the study area in A and C area. It was identified the deformations, called sliding surfaces, landslide furrows, scarps, collapsed zones, and cracks. If the areas of A and C are compared, the deformations are more in area C than in area A. Therefore, the risk of landslides may be higher in area C. In Fig. 8, the EM wave velocity calculated for the reflection surface in GPR5 cross-section -representing the GPR profiles- was shown as an example. The picks were exported with the attribute of two-way travel time and the velocity of propagation of the wave was calculated about 0.1 m/ns (Fig.

8). This value is generally observed in dry or wet soil, dry or wet clay and sandy environments (Wilchek, 2000; Cardomina, 2002). Therefore, it was thought that this velocity value was compatible with the geological units and electromagnetic waves led to rapid absorption due to the silty sandy clay layer. Because the first geological unit is medium-very stiff, low-high plasticity, silty sandy clay. The deformation structures as sliding surfaces, landslide furrows, scarps, collapsed zones, and cracks were observed in the GPR cross-sections (Fig. 8 and 9). In other words, the geological unit, the layer or topography slope and precipitation cause deformations in the loose upper unit. Therefore, these structures may develop or occur in the landslide mass, as shown in Fig. 8 and 9.

Additionally, the geological units were observed in DH wells in the geophysics study area (Fig. 4). These are mostly silty sandy clay and they have different characteristics above and below about 10 m in DH well. The topography of the study area decreases from 925 m to 840 m and the elevation difference is 85 m (Fig. 4). The amount of slope in the topography increases from south to north (>5^0-10^0) in the geophysical sections (Fig. 6 and 7). It was determined that the landslide type in the area was planar sliding and observed that the direction of sliding was SE. As this information was associated with topography and the field observations, it was observed that the topography was inclined from the north to the south of the study area. The results of the various studies and also the findings of this article have proved that Koyulhisar landslides are generally caused by the known reasons that trigger the landslide. Therefore, it was seen that the geological bedding was compatible with the topographical sloping and the groundwater was compatible with the direction of flow.

4 Conclusions

The landslides may develop under various geological, morphological, topographical and physical reasons. The information provided from many studies (geodetical, geological, morphological, seismological, topographic and meteorological) carried out across the region was compared with the geophysical results (SRT and GPR) and found to be compatible. The seismic P-wave velocity (V_P) of the layers, the tilt, tilt direction of the layers, depth of the sliding surface, sliding direction and the landslide type was determined from the geophysical sections. The study area was identified by the layers with the average seismic velocities of 650 < 1200 < 2100 <… m/sec. According to the geophysical cross-sections, it was identified that the depth of the sliding surface varied between 3-7 m due to the topographical differences. These depths were the depths with low seismic velocities (<650 m/sec) and defined as loose units which were also observed in geological drilling logs. It was determined that sliding surfaces, landslide furrows, collapsed zones, scarps, cracks were observed in the landslide mass in the GPR sections. It was observed that the layer tilt was generally more than 5^0 in all geophysical sections and compatible with the geology and the flow direction of the groundwater. It was determined that the landslide type in the area was planar sliding and the direction of sliding was SE.

The geophysical and other results were found to be compatible because it is known that the landslide direction across Koyulhisar is in S-SW and SE. Consequently, the fact that the depth of the sliding surface over the geologic unit is loose, the seismic velocity of the upper layer is low and the tilt is an excessive show that there is a new risk of landslide in the area. The other factors that trigger the landslide were found to be associated especially with the fact that the area is seismically active, receive heavy rain and has a poor vegetation cover. On the other hand, it was thought that blasting and excavation performed by human intervention can trigger the landslides due to the geologically loose unit. Hence, the landslide area can be a potential area which is open to natural/artificial hazards. The identified risks and natural hazards also threaten the settlement area, the buildings and other constructions (e.g. roads, walls, parks et al.) in Koyulhisar. Therefore, there is still a high landslide hazard in the study area and its surroundings, and this hazard will also occur in the future.

Acknowledgments: This study was supported by Cumhuriyet University Scientific Research Projects Commission as CÜBAP Project numbered M-464. We would like to thank Project Coordinator Assoc. Dr. Kemal Özgür Hastaoğlu and his research team, who allowed us to benefit from the results of TÜBİTAK (The Scientific and Technological Research Council of Turkey) supported project numbered 111Y111, for their contributions. We would like to thank Dr. Çağrı Çaylak for his contributions during the geophysical field measurements, Assoc. Dr. Fatih Poyraz for his contributions during the process of geodetic field measurements. We would like to thank Geological Engineer Mehmet Demirel for his contributions to the Fig. 2.

References

Aldaş, G. U., Kadıoğlu, S., Ulugergerli, E. U.: The effects of concealed discontinuities in blast design Pattern, 4th Int. Scientific and Technical Conference of Young Scientists and Specialists, St. Petersburg-RUSSIA, 6-7, 2003.

Annan, A. P., Davis, J.L., Gendzwill, D.: Radar sounding in potash mines: Saskatchewan, Canada, Geophysics, 53, 1556-1564, 1988.

Bano, M., Marquis, G., Niviere, B., Maurin, J. C., Cushing, M.: Investigating alluvial and tectonic features with ground penetrating radar and analyzing diffractions patterns, J. Appl. Geophys., 43, 3-41, 2000.

Benson, A. K.: Applications of ground penetrating radar in assessing some geological hazards: Examples of groundwater contaminants, faults, cavities, J. Appl. Geophys., 33, 177-193, https://doi.org/10.1016/0926-9851(95)90040-3, 1995.

Bichler, A., Bobrowsky, P., Best, M, Douma, M., Hunter, J., Calvert, T., Burns, R.: Three-dimensional mapping of a landslide using a multi-geophysical approach: the Quesnel Forks landslide, Landslides, 1, 29-40, DOI 10.1007/s10346-003-0008-7, 2004.

Bubeck, A., Wilkinson, M., Roberts, G. P., Cowie, P. A., McCaffrey, K. J. W., Phillips, R., Sammonds, P.: The tectonic geomorphology of bedrock scarps on active normal faults in the Italian Apennines mapped using combined ground penetrating radar and terrestrial laser scanning, Geomorphology, 237, 38-51, DOI:10.1016/j.geomorph.2014.03.011, 2015.

Cardimona, S.: Subsurface investigation using ground penetrating radar, Presented at the 2nd International Conference on the Application of Geophysics and NDT Methodologies Transportation Facilities and Infrastructure, Los Angels, California, 2002.

Davis, J. L., Annan, A. P.: Ground-penetrating radar for high resolution mapping of soil and rock stratigraphy, Geophys. Prosp., 37, 531-551, DOI: 10.1111/j.1365-2478.1989.tb02221.x, 1989.

Demir, G.: Landslide susceptibility mapping by using statistical analysis in the North Anatolian Fault Zone (NAFZ) on the northern part of Suşehri Town, Turkey, Nat. Hazards, 92, 133-154, https://doi.org/10.1007/s11069-018-3195-1, 2018.

Demirağ, O.: Jeofizik yöntemlerle heyelan araştırmaları, TMMOB-JFMO (The Chamber of Geophysical Engineers of Turkish) publications, Jeofizik, 5(1); 43-50, Ankara, Turkey, 1991 (in Turkish).

Demirel, M., Tatar, O., Koçbulut, F.: Kinematics of the faults around the Koyulhisar (Sivas) region on the North Anatolian Fault Zone, Geol. Bull., Turkey, 59(3),357-370, 2016 (in Turkish).

Duman, T. Y., Nefeslioğlu, H., Gökçeoğlu, C., Sönmez, H.: 17/03/2005 Kuzulu (Sivas-Koyulhisar) heyelanı, Maden Tetkik ve Arama Genel Müdürlüğü Jeoloji Etütleri Dairesi, Hacettepe Üniversitesi, 2005.

Gren, A., Gross, R., Holliger, K., Horstmeyer, H., Baldwin, J.: Results of 3D georadar surveying and trenching the San Andreas fault near its northern landward limit, Tectonophysics, 368, 7-23, doi:10.1016/S0040-1951(03)00147-1, 2003.

Gökçeoğlu, C., Nefeslioğlu, H. A., Sönmez, H., Duman, T., Can, T.: The 17 March 2005 Kuzulu landslide (Sivas, Turkey) and landslide-susceptibility map of its near vicinity, Eng. Geol., 81 (1), 65-83, DOI:10.1007/s00254-006-0322-1, 2005b.

Göktürkler, G., Balkaya, Ç., Erhan, Z.: Geophysical investigation of the landslide: The Altındağ landslide site, Izmir (western Turkey), J. Appl. Geophys., 65, 84-96, https://doi.org/10.1016/j.jappgeo.2008.05.008, 2008.

Hack, R.: Geophysics for slope stability, Surv. Geophys., 21, 423-338, 2000.

Harrari, Z.: Ground penetrating radar (GPR) for imaging stratigraphic features and groundwater in sand dunes, J. Appl. Geophys., 36, 43-52, https://doi.org/10.1016/S0926-9851(96)00031-6, 1996.

Hastaoğlu, K. O., Şanlı, D. U.: Monitoring Koyulhisar landslide using rapid static GPS: a strategy to remove biases from vertical velocities, Nat. Hazards, 58, 1275-1294, DOI:10.1007/s11069-011-9728-5, 2011.

Hastaoğlu, K. O.: Investigation of the groundwater effect on slow-motion landslides by using dynamic Kalman filtering method with GPS: Koyulhisar town center, Turkish J. Earth Sci., 1033-1046. DOI: 10.3906/yer-1210-10, 2013.

Hastaoğlu, K. Ö., Türk, T., Koçbulut, F., Balık Şanlı, F., Poyraz, F.: "GNSS ve PS-InSAR yöntemleri kullanılarak heyelanların izlenmesi ve afet bilgi sistemi tabanlı risk analizlerinin gerçekleştirilmesi: Koyulhisar (Sivas) heyelanları" Final report, TUBITAK Project Number: 111Y111, Program Code: 3501, www.tubitak.gov.tr, Turkey, 2015 (unpublished).

Hastaoglu, K. O.: Comparing the results of PSInSAR and GNSS on slow motion landslides, Koyulhisar, Turkey, Geomatics, Nat. Hazards and Risk, 7, 2, 786-803, DOI: 10.1080/19475705.2014.978822, 2016.

Hastaoglu K. O., Poyraz, F., Turk, T., Yılmaz, I., Kocbulut, F., Demirel, M., Sanli, U., Duman H., Balik Sanli, F.: Investigation of the success of monitoring slow motion landslides using Persistent Scatterer Interferometry and GNSS methods, Survey review 50, 363:475-486, DOI: 10.1080/00396265.2017.1295631, 2018.

Hatiboğlu, O.: Investigation of Koyulhisar (Sivas) Settlement area in terms of slope instability, Middle East Technical University, MS Thesis, Ankara, Turkey, 2009.

Hu, Z., Shan, W.: Landslide investigations in the northwest section of the lesser Khingan range in China using combined HDR and GPR methods, Bull. Eng.. Geol. Environ., 75, 591-603, DOI 10.1007/s10064-015-0805-y, 2016.

Lissak, C., Maquaire, O., Malet J.P., Lavigne, F., Virmoux, C., Gomez, C., Davidson, R.: Ground-penetrating radar observations for estimating the vertical displacement of rotational landslides, Nat. Hazards Earth Syst. Sci., 15, 1399-1406, doi:10.5194/nhess-15-1399-2015, 2015.

McCann, D. M., Forster, A.: Reconnaissance geophysical methods in landslide investigations, Eng. Geol. 29(1):59-78, https://doi.org/10.1016/0013-7952(90)90082-C, 1990.

MGM: Meteoroloji Genel Müdürlüğü (Turkish State Meteorological Service), Ankara Meteoroloji Bölge Müdürlüğü'nün Hidrotermal Şube Müdürlüğü (Hydrothermal Directorate of Ankara Meteorology Regional Directorate). https://www.mgm.gov.tr/ (accepted: 12.11.2008), 2016.

MTA: General Directorate of the Mineral Research and Exploration (MTA), (last access: 11.04.2018), http://yerbilimleri.mta.gov.tr/anasayfa.aspx, 2018.

Otto, J. C., Sass, O.: Comparing geophysical methods for talus slope investigations in the Turtmann valley (Swiss Alps), Geomorphology, 76, 257-272, doi:10.1016/j.geomorph.2005.11.008, 2006.

Över, D.: The Research of the landslide area ground of Koyulhisar district in Sivas with geophysical methods, Cumhuriyet University, MS Thesis, Sivas, Turkey, 2015.

Perrone, A., Iannuzzi, A., Lapenna, V., Lorenzo, P., Piscitelli, S., Rizzo, E., Sdao, F.: High-resolution electrical imaging of the Varco d'Izzo earthflow (southern Italy), J. Appl. Geophys., 56, 17-29, DOI:10.1016/j.jappgeo.2004.03.004, 2004.

Popescu, M., Şerban, R. D., Urdea, P., Onaca, A.: Conventional geophysical surveys for landslide investigations: Two case studies from Romania, Carpathian J. Earth and Environ. Sci., 11(1), 281-292, 2016.

Ristić, A., Abolmasov, B., Govedarica, M., Petrovački, D.: Shallow-landslide spatial Structure interpretation using a multi-geophysical approach, Acta Geotechnica, Slovenica, 47-59, 2012.

Sendir, H., Yılmaz, I.: Koyulhisar heyelanlarına yapısal ve jeomorfolojik açıdan bakış, Cumhuriyet Üniversitesi Mühendislik Fakültesi Dergisi, Seri A: Yer Bilimleri, 18 (1), 47-54, 2001 (in Turkish).

Sendir, H., Yılmaz, I.: Structural, geomorphological and geomechanical aspects of the Koyulhisar landslides in the North Anatolian Fault Zone (Sivas, Turkey), Environ. Geol., 42, 52-60, https://doi.org/10.1007/s00254-002-0528-9, 2002.

Slater, L., Niemi, T. M.: Ground penetrating radar investigation of active faults along the Dead Sea transform and implications for seismic hazards within the city of Aqaba, Jordan, Tectonophysics, 368, 33-50, 2003.

Su, L., Xu, X., Geng, X., Liang, S.: An integrated geophysical approach for investigating hydro-geological characteristics of a debris landslide in the Wenchuan earthquake area, Eng. Geol., http://dx.doi.org/10.1016/j.enggeo.2016.11.020, 2016.

Tatar, O., Gürsoy, H., Gökçeoğlu, C., Koçbulut, F., Duman, T. Y., Kök S., Süllü, H., Şenyurt, A., İleri, N.: 17 Mart 2005 Sivas ili Koyulhisar ilçesi Sugözü Köyü Kuzulu Mahallesi heyelanı 2. Değerlendirme raporu, http://www.koyulhisar.gov.tr/bulten3.doc., 2005 (in Turkish).

Tatar, O., Gürsoy, H., Altunel, E., Akyüz, S., Topal, T., Sezen , T. F., Koçbulut, F., Mesci, L., Kavak, K.Ş., Dikmen, Ü., Türk, T., Poyraz, F., Hastaoğlu, K., Ayazlı, E., Gürsoy, Ö., Polat, A., Akın, M., Demir, G., Zabcı, C., Karabacak, V., Çakır, Z.: Kuzey Anadolu Fay Zonu üzerinde Kelkit Vadisi boyunca yer alan yerleşim alanlarının doğal afet risk analizi, CBS tabanlı afet bilgi sistemi (KABİS) tasarımı: Proje tanıtımı ve ön bulgular. Aktif Tektonik Araştırma Grubu 11. Çalıştayı, TÜBİTAK-MAM Yer ve Deniz Bilimleri Enstitüsü Gebze-Kocaeli, Türkiye, 14-16, 2007 (in Turkish).

Terlemez, İ., Yılmaz A.: Ünye-Ordu-Koyulhisar-Reşadiye arasında kalan yörenin stratigrafisi, TJK Bülteni, 21, 179-191, 1980 (in Turkish).

Timothy, R. H., Davies, Warburton J., Stuart A. Dunning, Alodie, Bubeck, A. P.: A large landslide event in a post-glacial landscape: rethinking glacial legacy, Earth Surface Processes and Landforms, 38(11), 1261-1268, https://doi.org/10.1002/esp.3377, 2013.

Topal, T., Hatiboğlu, O.: Assessment of slope stability and monitoring of a landslide in the Koyulhisar settlement area (Sivas, Turkey), Environ. Earth Sci., 74(5), DOI 10.1007/s12665-015-4476-6, 2015.

Toprak, G. M. V.: Tectonic and stratigraphic characteristics of the Koyulhisar segment of the North Anatolian Fault Zone (Sivas-Turkey), METU (unpublished), Ph.D. Thesis, Ankara, Turkey, 121, 1989.

UDİM: Ulusal Deprem İzleme Merkezi (National earthquake monitoring center), Boğaziçi University KOERI (Kandilli Observatory And Earthquake Research Institute), www.koeri.boun.edu.tr/sismo/, (last access: 11.04.2018), Istanbul, Turkey, 2016.

Uysal, S.: Koyulhisar (Sivas) yöresinin jeolojisi, General Directorate of the Mineral Research and Exploration (MTA) Report number: 9838, 1995 (in Turkish).

Ulusay, R., Aydan, Ö., Kılıç, R.: Geotechnical assessment of the 2005 Kuzulu landslide (Turkey), Eng. Geol., 89(1-2), 112-128, 2007.

Wilchek, L.: Ground Penetrating Radar for Detection of Rock Structure, MS Thesis, Alberta University, Canada, 2000.

Yılmaz, I.: A case study from Koyulhisar (Sivas-Turkey) for landslide susceptibility mapping by Artificial Neural Networks, Bull. Eng. Geol. and the Environ., 68, 297-306, 2009.

Yılmaz, I., Ekemen T., Yıldırım, M., Keskin İ., Özdemir, G.: Failure and flow development of a collapse induced complex landslide: the 2005 Kuzulu (Koyulhisar, Turkey) landslide hazard, Environ. Geol., 49, 467-476, 2005.

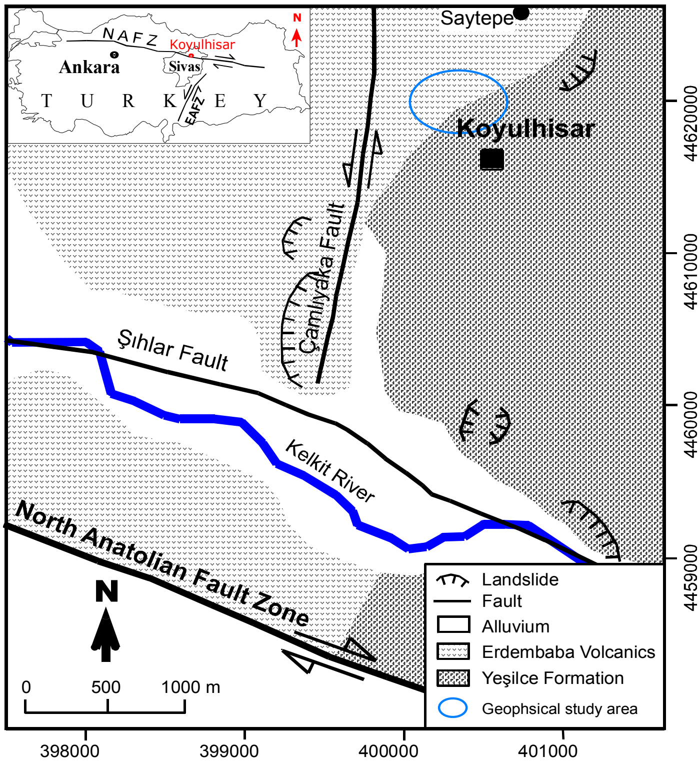

Figure 1. Geological map of study area. Arranged from Sendir and Yılmaz (2002) and Hastaoğlu (2016).

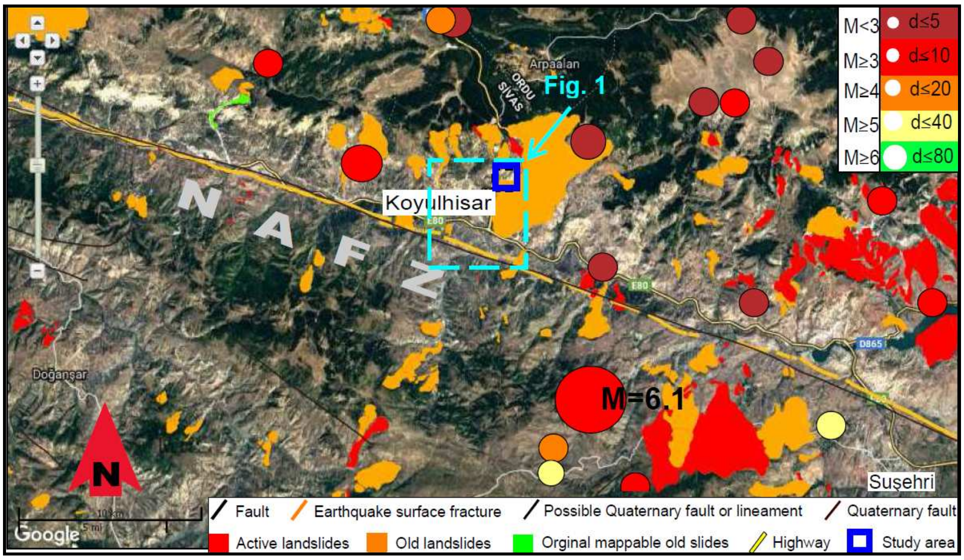

Figure 2. Seismic activity of the study area and its surroundings by the data between 1900-2015 years and the landslide areas (UDIM, 2016; MTA, 2018).

Table

Table 1. The annual average meteorological values of Sivas by years between 1950-2015 (MGM, 2016).

SIVAS	January	February	March	April	May	June	July	August	September	October	November	December
The average tempreture (^{0}C)	-3.2	-2.0	2.9	9.1	13.5	17.2	20.2	20.2	16.2	10.8	4.6	-0.6
The average the highest tempreture (^{0}C)	1.0	2.6	8.1	15.3	20.0	24.0	27.9	28.5	24.7	18.4	10.6	3.7
The average the lowest tempreture (^{0}C)	-7.0	-6.2	-1.7	3.4	7.2	9.9	12.0	11.9	8.3	4.4	-0.2	-4.2
The average sunshine duration (hour)	2.3	3.3	4.5	6.2	8.1	10.4	12.1	11.4	9.4	6.3	4.1	2.3
The average number of rainy days	13.0	12.4	13.7	14.0	14.4	8.8	2.5	2.1	4.3	8.0	9.5	12.1
The average monthly total rainfall (kg/m^2)	42.0	40.3	46.0	59.1	60.7	34.8	8.5	5.9	16.9	32.9	41.0	44.2
The highest and the lowest values occurring over many years (1950-2015)												
The highest tempreture (^{0}C)	14.6	18.1	25.2	29.0	32.0	35.5	40.0	39.4	35.7	30.5	22.8	19.4
The lowest tempreture (^{0}C)	**-34.6**	**-34.4**	**-27.6**	**-10.9**	**-4.2**	**-0.3**	**3.4**	**3.2**	**-3.8**	**-8.1**	**-24.4**	**-27.0**
Daily total the highest rainfall	**2 May 1991**	**55.0 kg/m^2**	Daily the fastest wind			**5 Jan. 1996**		**122.8 km/h**	**The highest snow**		**2 Feb. 1950**	**110.0 cm**

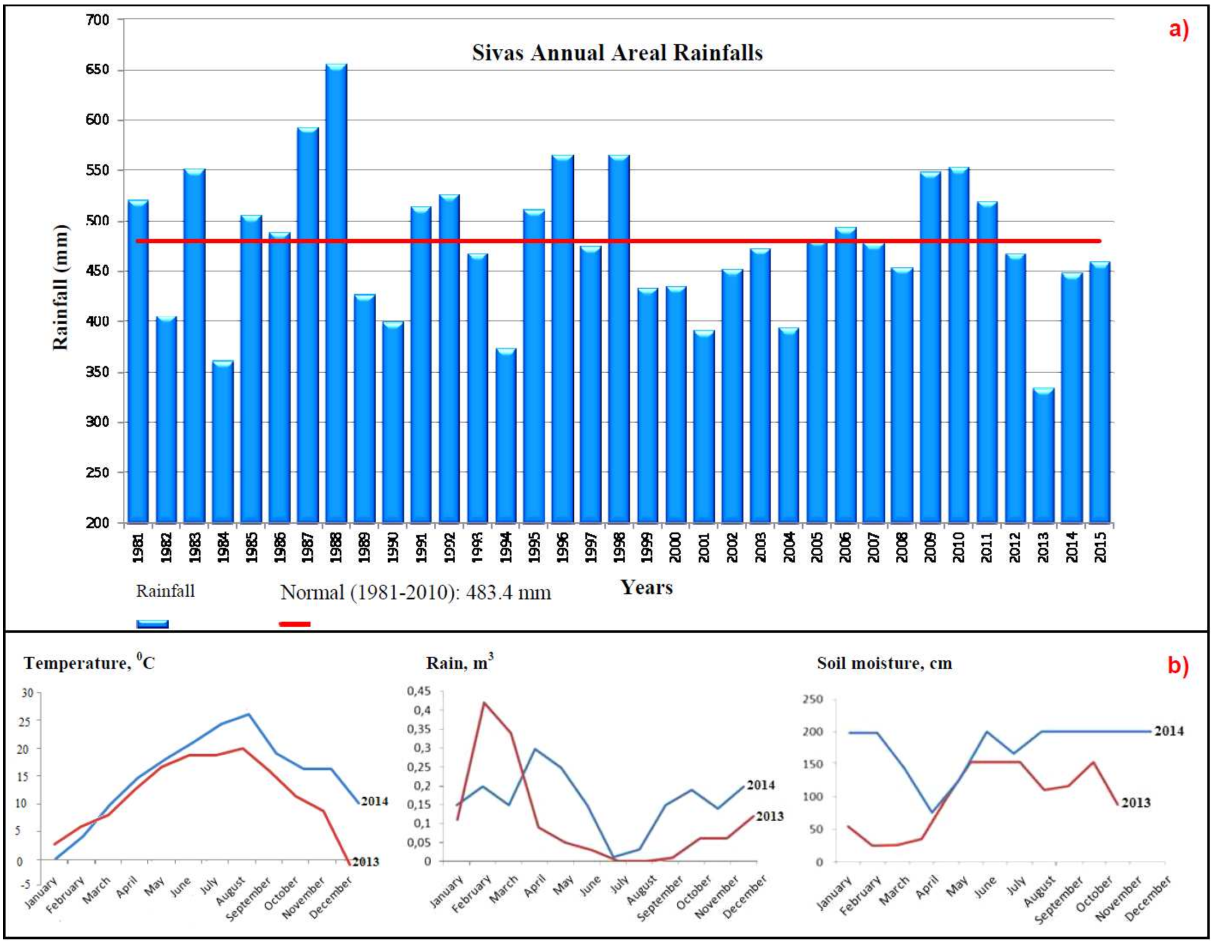

Figure 3. a) Precipitation distribution in between 1981-2015 years of Sivas (MGM, 2016). **b)** Graphics of monthly average temperature (T, ^{0}C), rainfall (m^3) and soil moisture content (cm) of the study area and its surroundings in the years of 2013 and 2014. They were prepared from the project data (Hastaoğlu et al., 2015).

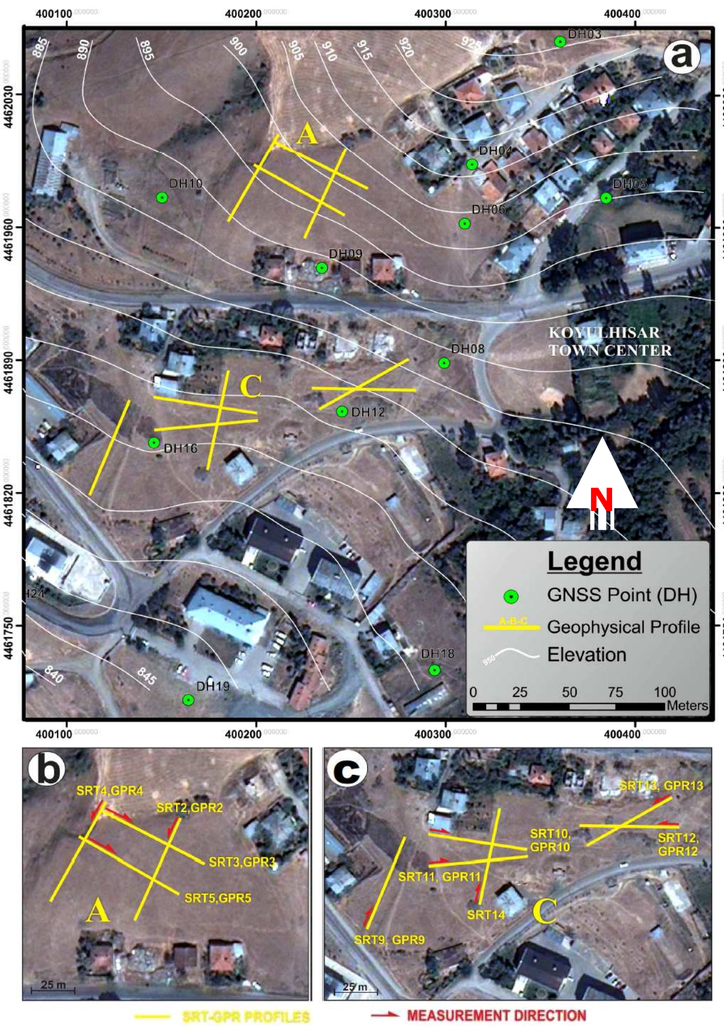

Figure 4. (a) The study area. (b) and (c) The details of geophysics profiles for the A and C areas.

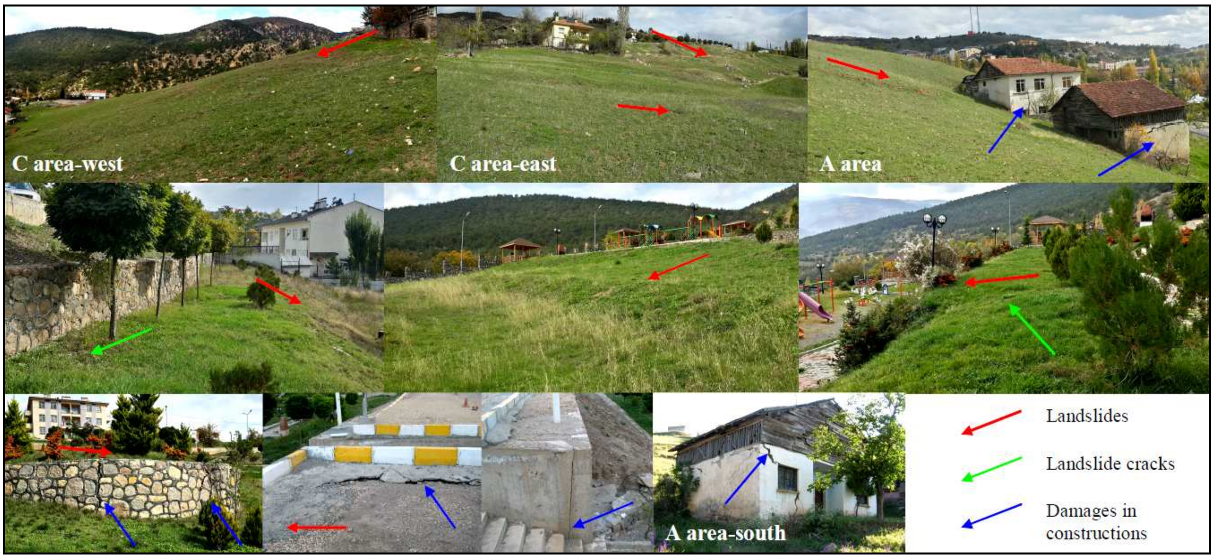

Figure 5. The photos of the study area and its surroundings, in which the landslides, landslide cracks or constructional damages are also observed.

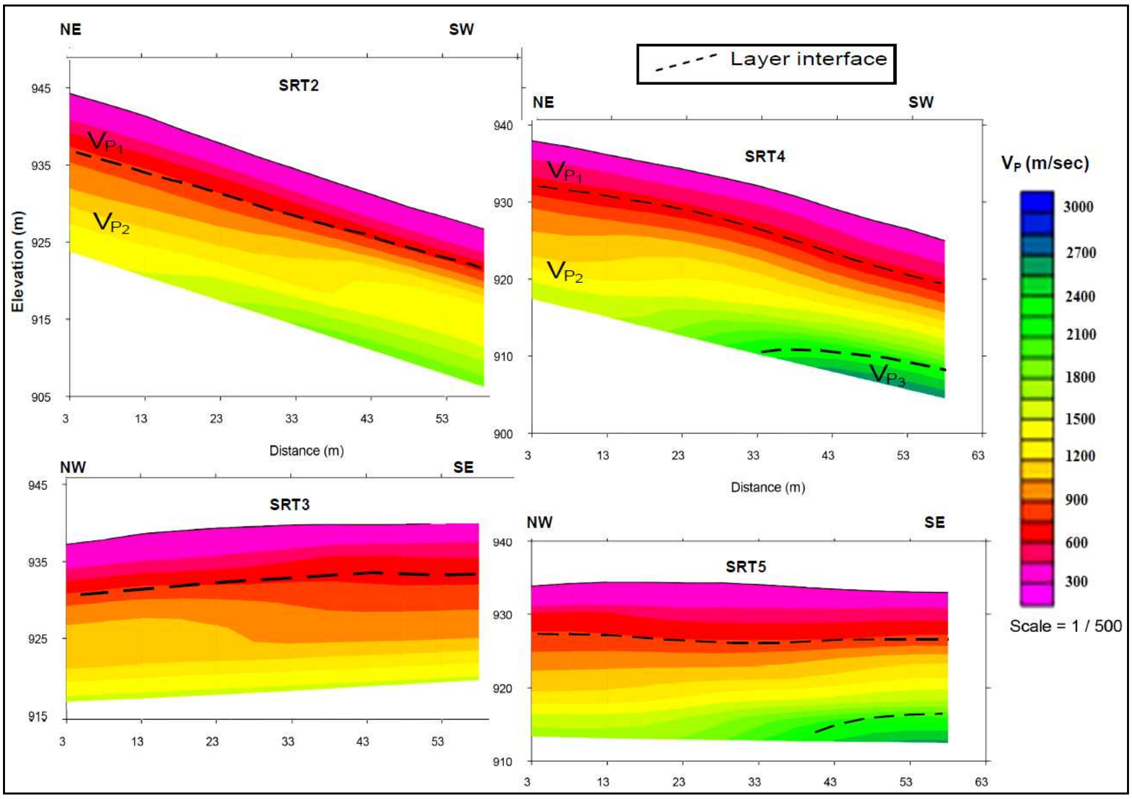

Figure 6. The seismic profiles of the area **A**. The uppermost boundary of the V_{P2} layer is the depth of the sliding surface (This depth changes between ~3-7 m). The lower velocity V_{P1} layer consists of soil and alluviums (the average seismic V_{P1}< 650 m/sec).

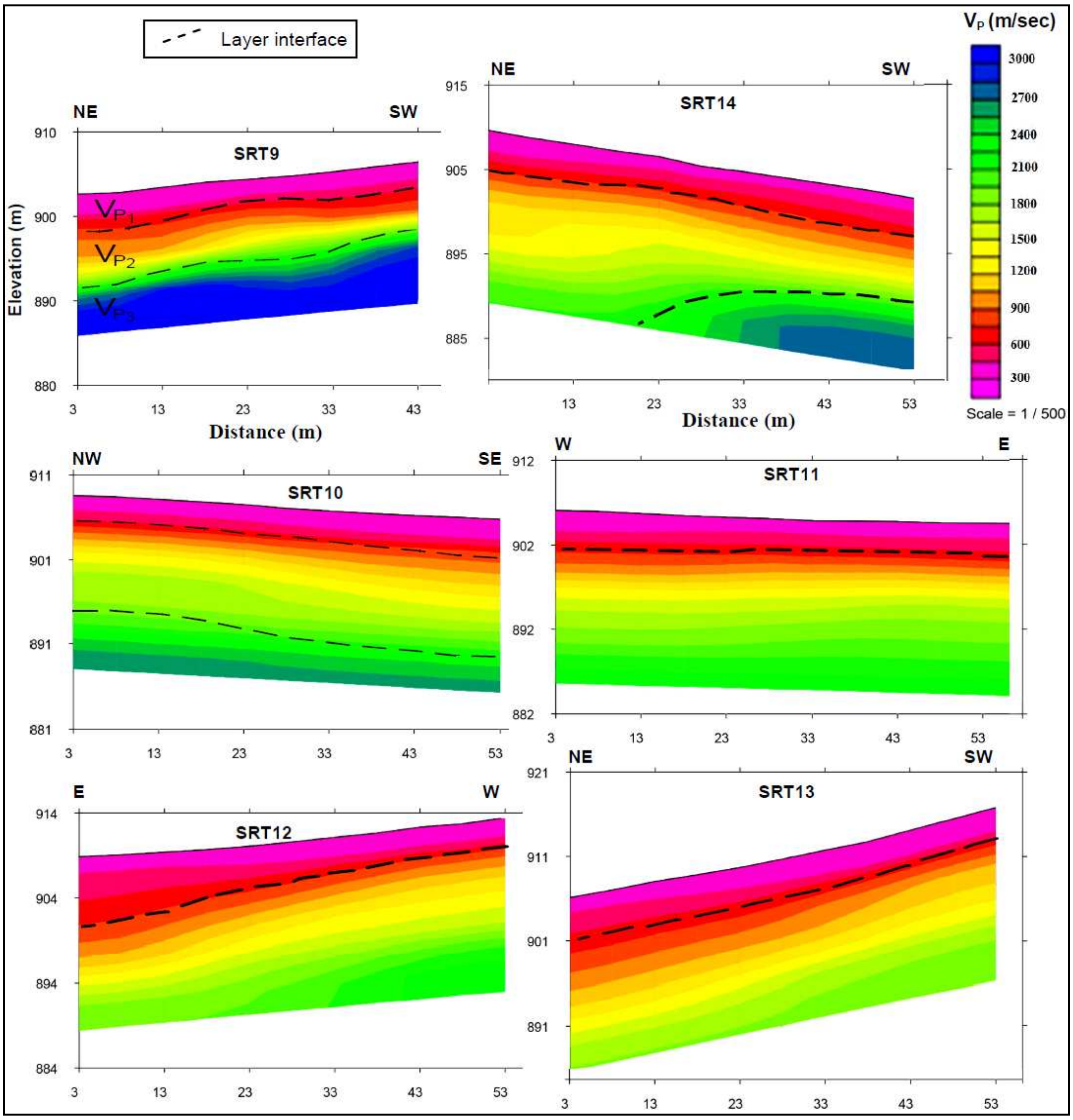

Figure 7. The seismic profiles of the area **C**. The uppermost boundary of the V_{P2} layer is the depth of the sliding surface (This depth changes between ~3-7 m). The lower velocity V_{P1} layer consists of soil and alluviums (the average seismic V_{P1}< 650 m/sec).

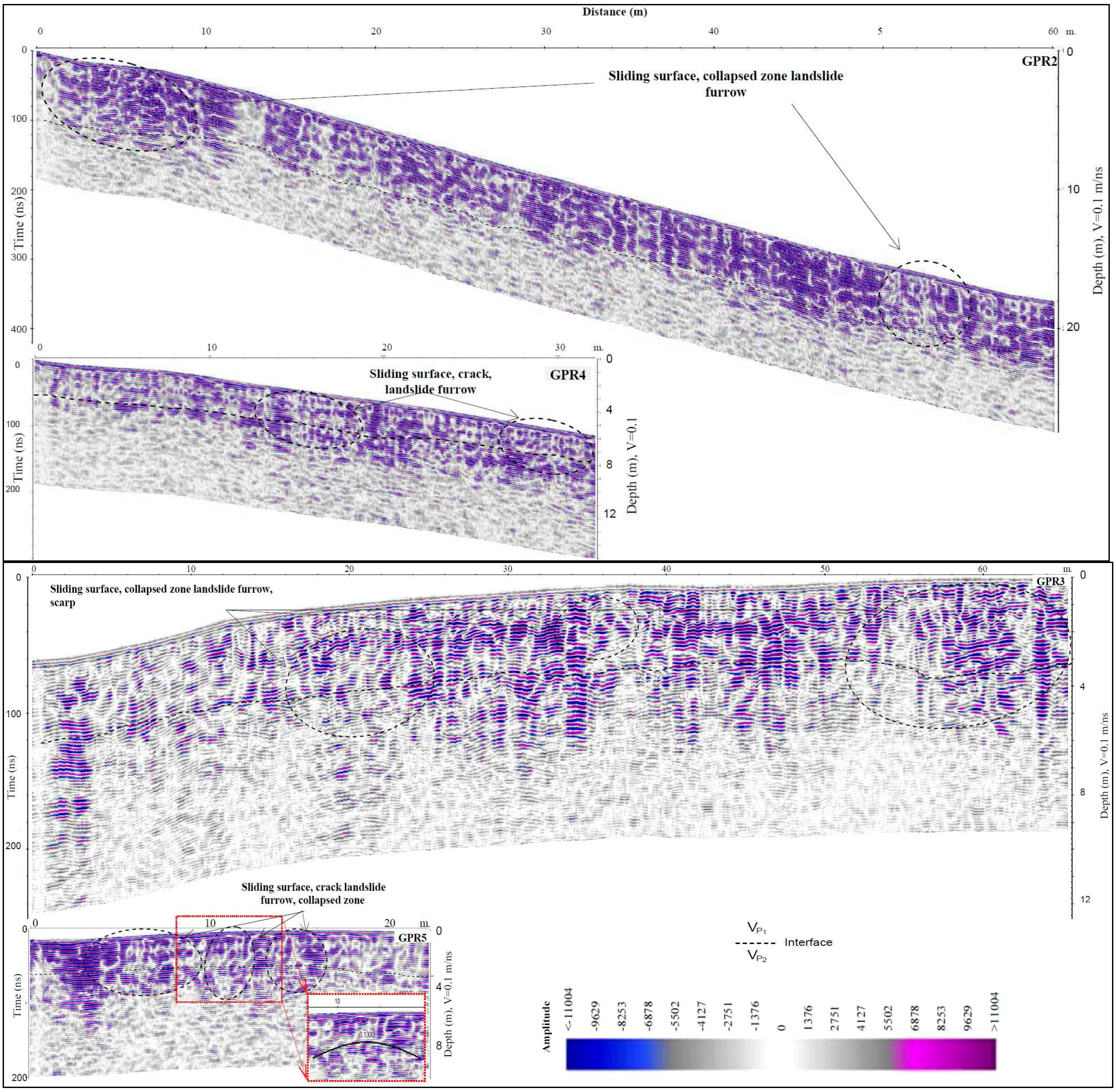

Figure 8. GPR profiles in A area and the deformations in the loose layers (the seismic V_{P1} layer).

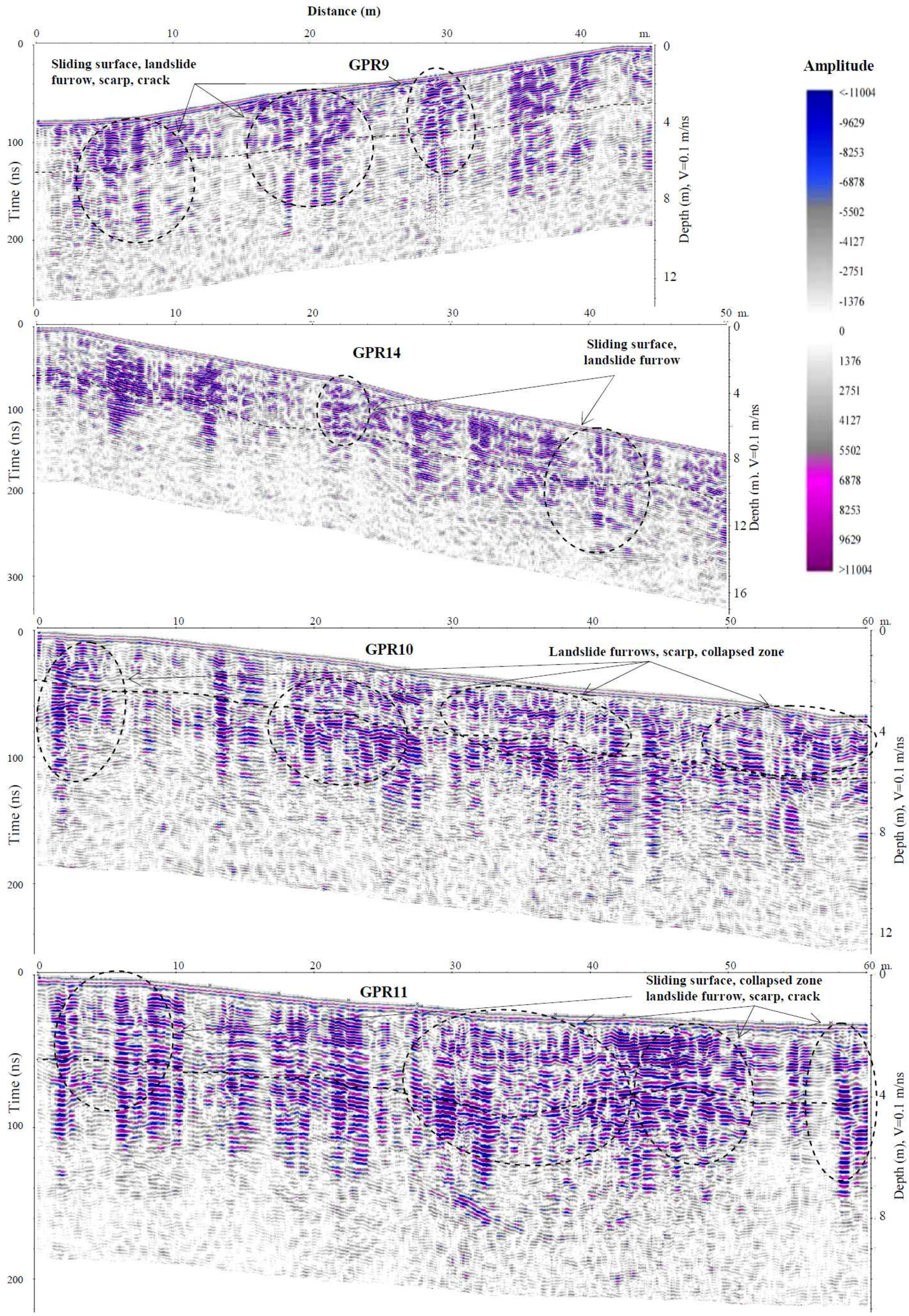

493

494 **Figure 9.** GPR profiles in the C-west area and the deformations in the loose layer (the seismic V_{P1} layer).

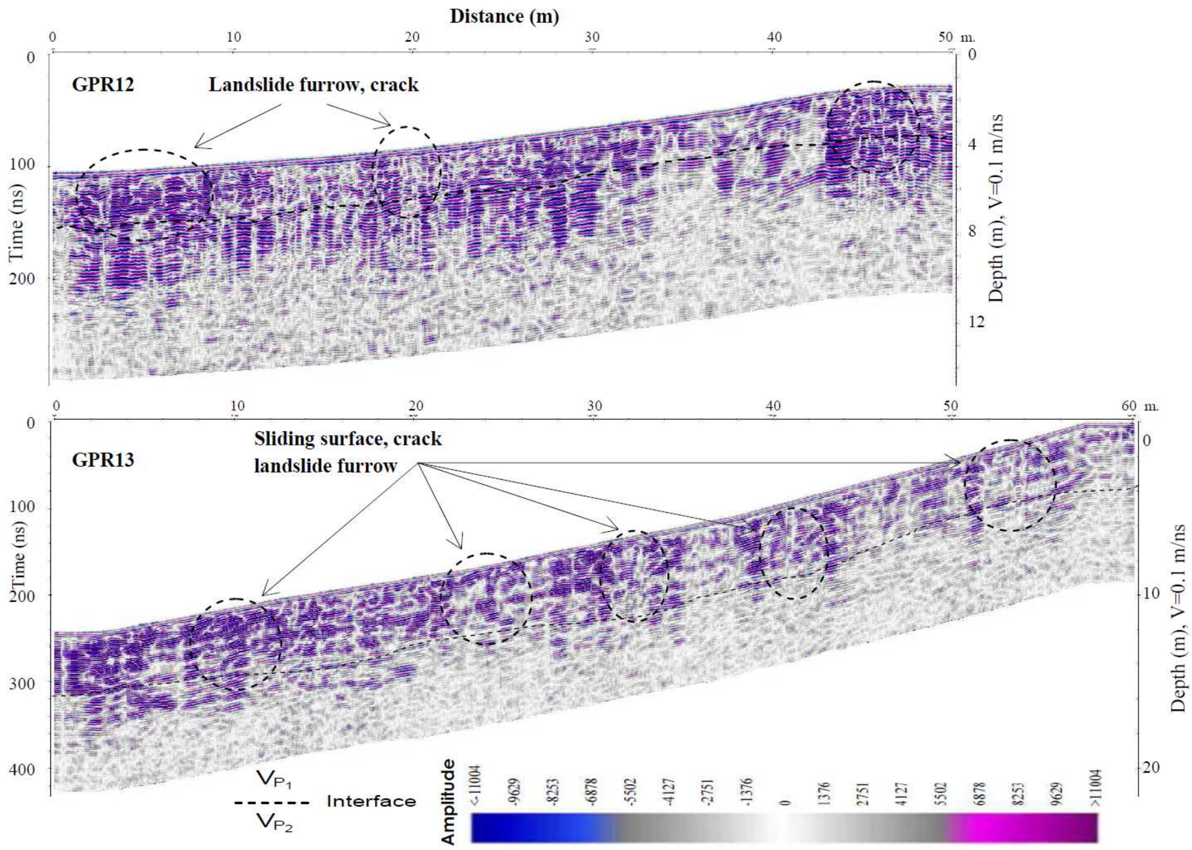

Figure 9. (…contiune) C-east area.